A Maximum Power Point Tracking System With Parallel Connection for PV Stand-Alone Applications

Roger Gules, Juliano De Pellegrin Pacheco, Hélio Leães Hey, *Member, IEEE*, and Johninson Imhoff

***Abstract*—This paper presents the analysis, design, and implementation of a parallel connected maximum power point tracking (MPPT) system for stand-alone photovoltaic power generation. The parallel connection of the MPPT system reduces the negative influence of power converter losses in the overall efficiency because only a part of the generated power is processed by the MPPT system. Furthermore, all control algorithms used in the classical series-connected MPPT can be applied to the parallel system. A simple bidirectional dc–dc power converter is proposed for the MPPT implementation and presents the functions of battery charger and step-up converter. The operation characteristics of the proposed circuit are analyzed with the implementation of a prototype in a practical application.**

***Index Terms*—DC–DC power conversion, photovoltaic (PV) power systems, solar energy.**

I. Introduction

THE CONTINUOUS growth of the global energy demand associated with society's increasing awareness of environmental impacts from the widespread utilization of fossil fuels has led to the exploration of renewable energy sources, such as photovoltaic (PV) technology. Although PV energy has received considerable attention over the last few decades, the high installation cost of PV systems and the low conversion efficiency of PV modules are the major obstacles to using this alternative energy source on a large scale. Therefore, several studies are being developed in order to minimize these drawbacks [1]–[9]. In order to extract the maximum power of the PV array, the classical implementation of the maximum power point tracking (MPPT) in stand-alone systems is generally accomplished by the series connection of a dc–dc converter between the PV array and the load or the energy storage element. Considering that in the series connection, the dc–dc converter always processes all power generated, the total efficiency of the PV system greatly depends on the efficiency of this series dc–dc converter. As an alternative to this configuration, this paper presents an MPPT system based on the parallel connection of a dc–dc converter. With this configuration, only a part of the energy generated is processed by the dc–dc converter, making it possible to obtain an increase in the total efficiency of the PV system as compared with the series configuration.

The operation principle, theoretical analysis, design methodology, and experimental results of a laboratory prototype of the parallel MPPT system are presented in this paper.

Manuscript received September 26, 2007; revised March 31,2008. This work was supported by Fundação Araucária under Grant 10966.

R. Gules and J. D. P. Pacheco are with the Federal University of Technology CPGEI-UTFPR, 80230-901 Curitiba, Brazil (e-mail: rgules@gmail.com).

H. L. Hey is with the Power Electronics and Control Research Group, Federal University of Santa Maria, Santa Maria 97105-900, Brazil.

J. Imhoff is with the Electrolux do Brazil S.A., Curitiba 81520-900, Brazil.

Digital Object Identifier 10.1109/TIE.2008.924033

II. MPPT in Stand-Alone PV Systems

A. Solar Cell Output Characteristic

The maximum power of the PV module changes with climatic conditions, and there is only one value for the current ($I_{\rm mpp}$) and the voltage ($V_{\rm mpp}$), which defines the maximum power point (MPP), as shown in Fig. 1 [1]–[3]. The PV current changes with the solar irradiation level, whereas the PV output voltage changes with the temperature of the PV module. Therefore, an important challenge in a PV system is to ensure the maximum energy generation from the PV array with a dynamic variation of its output characteristic and with the connection of a variable load. A solution for this problem is the insertion of a power converter between the PV array and load, which could dynamically change the impedance of the circuit by using a control algorithm. Thus, MPP operation can be obtained under any operational condition.

B. Series Connection of the MPPT

The classical implementation of the MPPT is the series connection of a dc–dc converter between the source and load, which is as shown in Fig. 2 and which presents both functions of battery charger and MPPT.

In order to obtain a good dynamic performance from the MPPT, different control algorithms were developed [4]–[8]. With data for the actual power extracted from the PV array, which are obtained by measuring the voltage and current in the PV array, the task of these algorithms is to change the converter duty cycle in order to reach the MPP.

The practical implementation of the MPPT algorithm is normally accomplished through a digital system, which uses a microcontroller or DSP.

As shown in Fig. 2, the dc loads can be directly supplied from the battery bank. If it is necessary to supply ac loads, a step-up dc–dc converter must be utilized in order to increase the battery bank voltage to the required dc bus level, which is necessary for generating 110/220 $V_{\rm ac}$ output voltage from

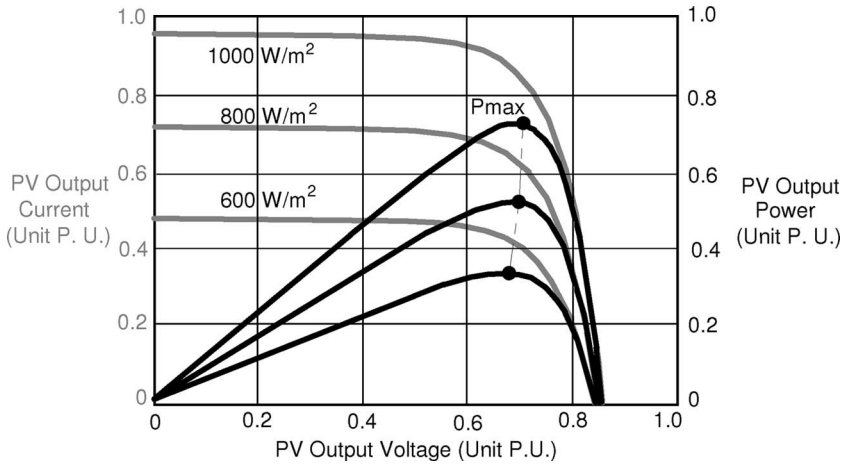

Fig. 1. Output characteristic of a PV module.

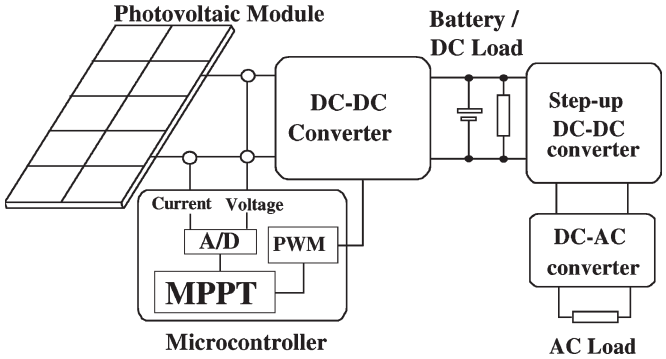

Fig. 2. MPPT system with series connection.

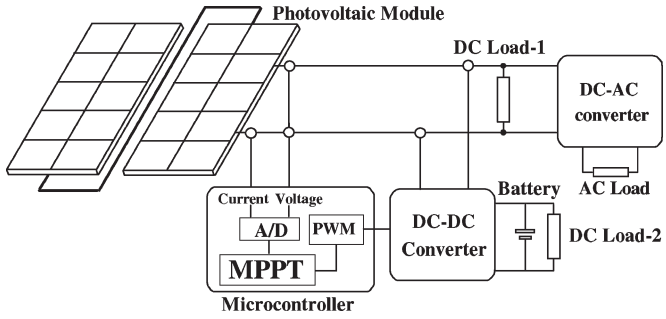

Fig. 3. MPPT systems with parallel connection.

a dc–ac converter. As there are several converters that are in series with this configuration, its overall efficiency greatly depends on the efficiency of each converter. Therefore, the efficiency of each stage must be optimized in order to avoid an excessive decrease in efficiency, which would increase the implementation cost and the number of PV modules.

C. Parallel Connection of the MPPT

Fig. 3 shows an alternative proposal to implement stand-alone PV power generation based on a parallel MPPT system. The parallel connection of the MPPT circuit was introduced in [9], and the main advantage of this configuration is that the dc–dc converter processes only a part of the generated power, allowing for higher efficiency as compared with the series configuration. In line with this concept, an integrated power circuit is proposed in this paper with the following multiple functions: battery charge, battery regulator, and step-up converter. The best operation condition occurs when the load current value is equal to the PV module MPP current value (I_{mpp}), where the dc–dc converter does not process power.

Depending on the dc load voltage level, the dc loads can be connected in parallel with the PV module ("DC Load-1") and/or in parallel with the battery bank ("DC Load-2"). However, the voltage level of the PV module is higher than the battery voltage. If the system must also supply the ac loads, a dc–ac converter can be connected in parallel with the PV modules, as shown in Fig. 3. In this case, an output transformer can be used to generate the nominal ac voltage, or additional PV modules can be added in a series connection in order to obtain the dc voltage level that is necessary to generate the nominal ac voltage. As can be seen, two conversion stages between the PV modules and the output inverter are eliminated in the proposed parallel stand-alone system when compared with the series stand-alone system.

This may represent a significant increase in the overall efficiency and reliability of the system, which is besides enabling a reduction in the cost of the electronic system utilized. On the other hand, the series connection of a higher number of PV modules would present a significant reduction in the energy generated and could make it difficult to obtain the MPP in cases of shading/defect of one or more PV modules.

The output characteristic of two PV modules under two different sunlight conditions is shown in Fig. 4. The black curve represents the output characteristic of the module operating with total solar irradiation, and the gray curve represents the output characteristic of a shaded module operating with partial solar irradiation. Fig. 5 shows the equivalent output characteristic of PV modules connected in series, where one module operates with partial solar irradiation. Besides the reduction of the maximum power, the classic MPPT algorithms may create difficulty in reaching the MPP due to the existence of two power peak values. The configuration shown in Fig. 6 can not only generate a high dc voltage but can also solve the problems of the series connection of the PV module. The proposed parallel

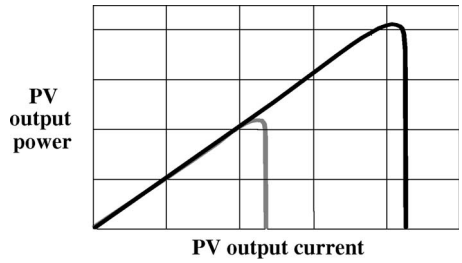

Fig. 4. Output curve of (gray line) shaded and (black line) unshaded PV modules.

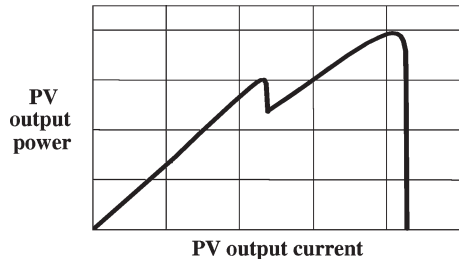

Fig. 5. Output curve of the series-connected PV modules with different solar irradiation.

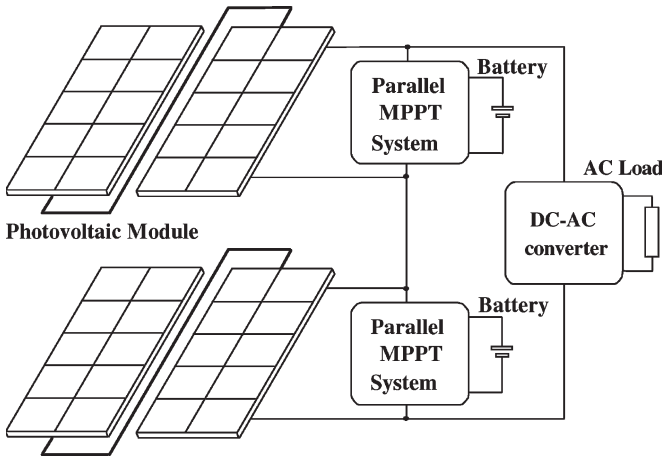

Fig. 6. Series connection of multiple parallel MPPT and dc–ac converter.

MPPT circuit presents a modular characteristic, and two or more circuits can be connected in series, obtaining a high dc voltage. Each MPPT circuit can provide an individualized MPPT, reducing the effects of the shading/failure of PV modules and maximizing the energy generated by the system.

III. Proposed MPPT Controller

A. Power Circuit Operation

In order to verify the operation characteristics of the proposed parallel MPPT system shown in Fig. 7, only a dc load connected in parallel with the PV module was considered (Fig. 3, "DC Load-1"). It was composed of a battery bank storage energy, (C) a capacitor, (L) an inductor, and a power semiconductor leg (S_1-D_1 and S_2-D_2). The bidirectional converter operates as a buck converter in the battery charge mode and as a boost converter when the battery must supply the load (R_L) or when the load energy demand is higher than the energy generated. The converter duty cycle is generated by the same control algorithms that are used in the series-connected MPPT. The operation analysis of the proposed converter is presented for use with hard-switching pulsewidth modulation. However, it must be highlighted that the power circuit efficiency can be improved by using soft-switching techniques [14], [15].

1) Buck Operation Mode: Fig. 8 shows the two topological stages that occur during the buck operation mode. The battery bank voltage must be lower than the PV module voltage for correct operation. When the energy generated is enough to supply the load, the exceeding energy is used to charge the battery. When the power switch S_1 is turned on, the inductor L stores energy, and the energy flows from the PV module to the battery bank. When the power switch S_1 is turned off, the diode D_2 conducts, and the energy stored in the inductor L is transferred to the battery. The switches' command signals are complementary, and therefore, the switch S_2 is turned on during the conduction of the diode D_2.

2) Boost Operation Mode: If the energy generated at the MPP is not enough to supply the load, the power system operates as a boost converter, transferring energy from the battery to the load. In this case, while the switch S_2 is turned on, the inductor L stores energy from the battery, as shown in Fig. 9. When the switch S_2 is turned off, the energy stored in the inductor is transferred to the load. Fig. 10 shows the command signal of the power switches $S_1(V_{CS1})$ and $S_2(V_{CS2})$ and the inductor current waveform (I_L) in the buck and boost operations.

The greatest advantage of the proposed parallel MPPT system with a bidirectional power circuit, which is as shown in Fig. 7, is the integration of multiple functions in a single cost-effective converter, which combines simplicity, reliability, and low cost. The multiple functions of the proposed system are as follows: battery bank charger, which is when the energy generated by the PV array is higher than the load consumption; MPPT controller, which is in order to extract the maximum energy from the PV array; and step-up dc–dc converter, which is when the energy of the PV array is not enough to supply the load. The control algorithm ensures the operation of the PV module at the MPP, implementing the MPPT function.

The battery charge state is also observed by the digital control system, which avoids battery overcharge or excessive discharge in order to prolong the battery life time.

B. System Operation Modes

The basic circuit of the parallel MPPT system can present five operation modes considering climatic conditions and load variation. Figs. 11–15, present the operation modes, and for the purpose of simplification, the PV module is represented by a current source (I_f).

1) Operation Without Load $(I_c = 0)$*—Mode 1 (Fig. 11):* When the load is not connected, the battery is charged with the PV module current ($I_f = I_b$, and $I_c = 0$). The MPPT algorithm ensures that the converter current (I_b) is equal to the PV module MPP current (I_{mpp}).

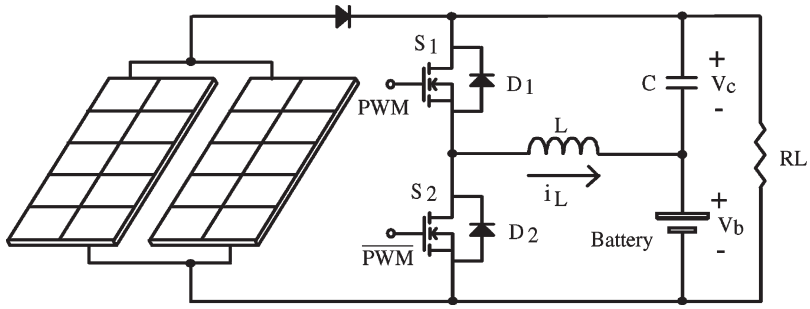

Fig. 7. MPPT system with bidirectional dc–dc converter.

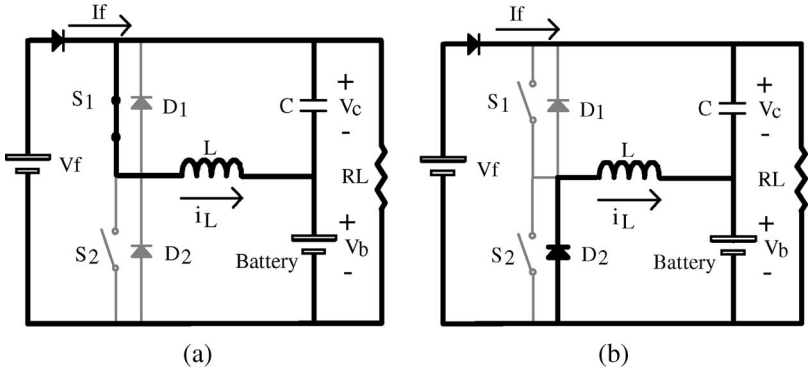

Fig. 8. Buck operation mode. (a) S_1 turned on. (b) S_1 turned off.

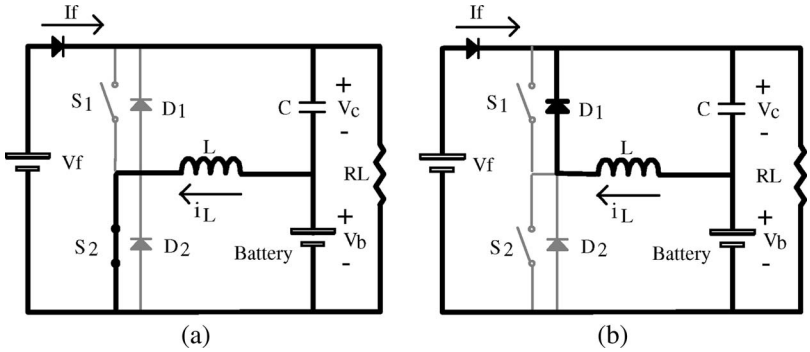

Fig. 9. Boost operation mode. (a) S_2 turned on. (b) S_2 turned off.

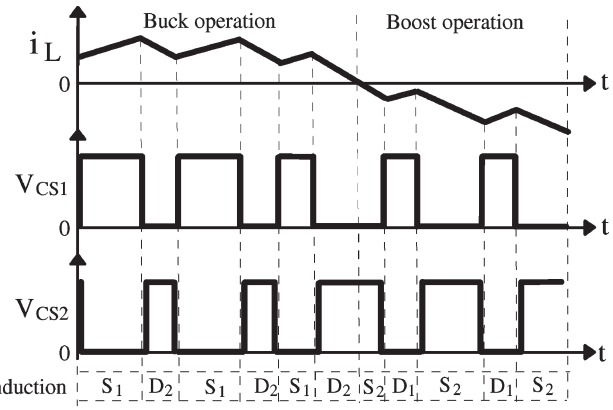

Fig. 10. Bidirectional operation of the inductor current.

In addition, the sum of the battery and the capacitor voltages $(V_b + V_c)$ is equal to the PV module MPP voltage (V_{mpp}). The system operates as a buck converter to charge the battery.

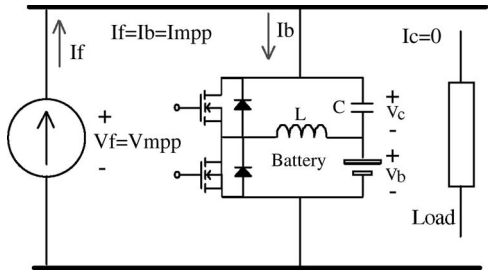

Fig. 11. Operation mode 1.

2) Operation With Load Current That is Lower Than the MPP Current $(I_c < I_{mpp})$*—Mode 2 (Fig. 12):* If the load current value (I_c) is lower than the PV module MPP current (I_{mpp}), part of the energy generated by the PV module is used to supply the load, and another part is used to charge the battery. The control algorithm maintains the sum of the load current and the converter current equal to the MPP current

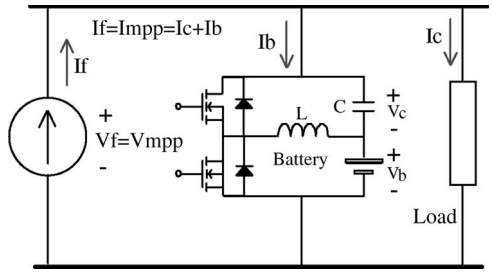

Fig. 12. Operation mode 2.

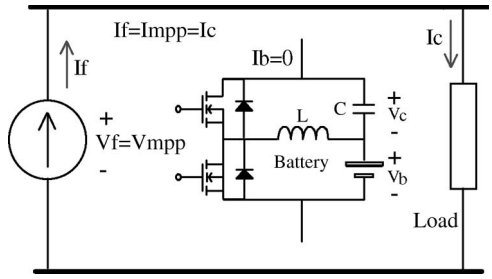

Fig. 13. Operation mode 3.

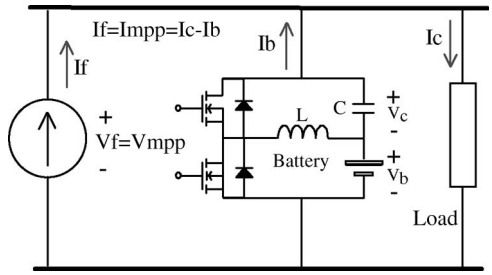

Fig. 14. Operation mode 4.

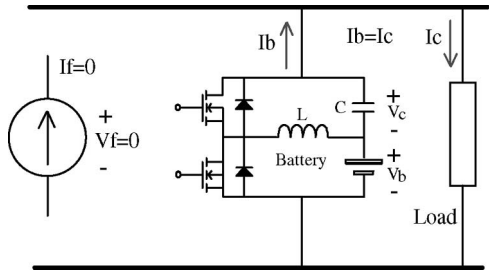

Fig. 15. Operation mode 5.

$(I_f = I_{\rm mpp} = I_{\rm c} + I_{\rm b})$. The system operates as a buck converter to charge the battery.

3) Operation With Load Current That is Equal to the MPP Current $(I_{\rm c} = I_{\rm mpp})$*—Mode 3 (Fig. 13):* When the load current value $(I_{\rm c})$ is equal to the PV module MPP current $(I_{\rm mpp})$, the power processed by the dc–dc converter is zero. In this case, the efficiency of the power system can be considered close to 100% because the maximum power of the PV module is transferred to the load without any power processing by the dc–dc converter.

4) Operation With a Load Current That is Higher Than the MPP Current $(I_{\rm c} > {\rm I}_{\rm mpp})$*—Mode 4 (Fig. 14):* If the load current value $(I_{\rm c})$ is higher than the PV module MPP current $(I_{\rm mpp})$, all energy generated by the PV module is supplied to the load. The additional power that is necessary to complement the load power must be supplied by the dc–dc converter. The control algorithm maintains the PV module current at the MPP $(I_f = I_{\rm mpp} = I_{\rm c} - I_{\rm b})$. The battery is discharged during this operation mode, and the dc–dc converter operates as a boost converter.

5) Operation Without Solar Irradiation $(I_f = 0)$*—Mode 5 (Fig. 15):* The dc–dc converter supplies the load during operation without solar irradiation or under shading. In this case, the MPPT algorithm is disabled, and a digital voltage control loop regulates the load voltage.

The battery is discharged during this operation mode, and the dc–dc converter operates as a boost converter, considering the battery as the input source. The control system also verifies the battery discharge state and must turn off the dc–dc converter when the battery energy level reaches its lowest limit.

C. Control Algorithms

The control strategy of the proposed system is composed of different algorithms, which must control the MPPT process (operation modes 1, 2, and 4), the charge process of the battery bank (operation modes 1 and 2), and the output voltage regulation (operation mode 5).

1) MPPT Algorithm: The PV voltage and current are monitored, and the PV power can be controlled as in the series-connected system. There are many studies that analyze the energy efficiency of different MPPT algorithms, and several control algorithms with different performances are presented in the literature [4]–[8]. The transition between the different operation modes must occur without discontinuity of the load in the parallel-connected MPPT system. The convergence time of the MPPT algorithm is, normally, not important for the series-connected system because the climatic transitions occur with a high constant time and because the load is connected to the battery bank. However, the utilization of a fast convergence MPPT algorithm is important for the parallel system in order to minimize the transient in the output voltage with the load variation. As the analysis of the MPPT algorithm was not the focus of this paper, the perturbation and observation method was utilized, and the control algorithm is shown in Fig. 16. The sample of the PV module voltage $V_{f(n)}$ and current $I_{f(n)}$ are used to calculate the instantaneous power $P_{f(n)}$. The power obtained in the last iteration $P_{f(n)}$ is compared with the power calculated in the previous iteration $P_{f(n-1)}$. In addition, the value of the duty cycle at the last iteration $D_{(n)}$ is compared with the previous duty cycle $D_{(n-1)}$ in order to ascertain whether the converter duty cycle must be increased or decreased in order to reach the MPP.

2) Battery Charge Control: While the PV module generates energy, the MPPT algorithm is active and maintains the PV module operating with maximum power. If the PV current is higher than the load current, the battery bank is charged with the difference between these currents. The PV module presents a current source output characteristic at the maximum current value, as shown in Fig. 1. Therefore, if the maximum PV current is considered in the design of the battery bank, a current control loop is not necessary to limit the maximum battery charge current. The highest battery charge current occurs

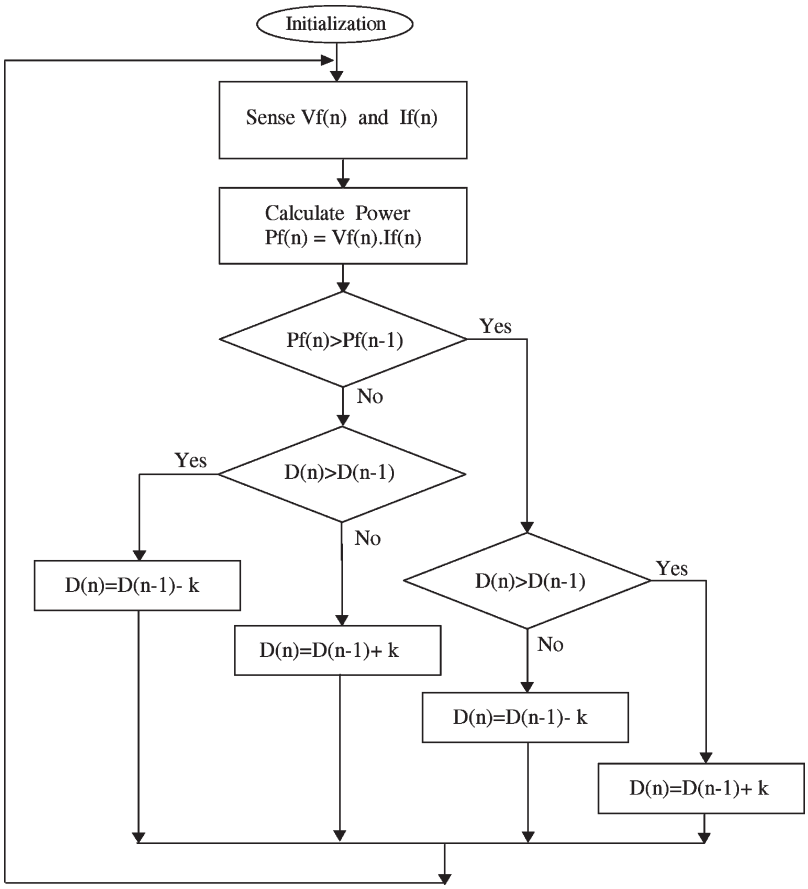

Fig. 16. Perturbation and observation control algorithm.

when the system operates with maximum solar irradiation and without load. When PV-generated energy is lower than the load demand, the necessary additional energy is supplied by the battery bank. Thus, the charge or discharge battery current is controlled by the MPPT algorithm. During the operation of the MPPT algorithm, the battery state of charge is verified, and when the state of charge reaches its lowest level, the battery discharge function is disabled, and the system is turned off. In addition, when the battery state of charge reaches its highest limit level, the MPPT algorithm is disabled, and the output voltage control loop is enabled (operation mode 5). In this case, the reference voltage adopted for the constant voltage control loop must define an output voltage that is close to the PV MPP voltage but higher in order to allow for the battery discharge. After a small partial battery discharge, the MPPT algorithm returns to operation, and a cyclic transition between the MPPT and voltage regulation algorithm occurs while the battery is fully charged and the energy generated is higher than the load energy demand. The control algorithm developed for the parallel MPPT operates only with the battery bank connected to the system.

3) Voltage Control Loop: The voltage control loop is also activated when the energy from the PV module is very low or null. In this case, the MPPT algorithm is disabled, the dc–dc power circuit operates as a boost converter, and the battery bank supplies the load with a constant voltage. In this situation, the reference voltage defined in the control algorithm is compared with the output voltage, and the error signal is applied to the digital voltage compensator. The control action defines the converter duty cycle in order to regulate the output voltage. The voltage reference considered is equal to 15 V, which is the intermediate value of the MPP voltage of the PV module utilized in the practical implementation. As occurs with the MPPT algorithm during the voltage control loop operation, the battery state of charge is verified, and the system is turned off when the battery reaches its lowest level.

D. Design Parameters

The MPP voltage (V_{mpp}) of the PV module utilized in the practical implementation is between approximately 12.5 and 17.5 V for typical climatic conditions, and the battery voltage must be lower in order to allow for the operation of the power circuit in the buck and boost operation modes. The battery utilized in the practical implementation presents a nominal voltage that is equal to 6 V. The continuous conduction mode operation is considered in the determination of the main prototype components, which is based on the circuit shown in Fig. 7. The components and semiconductors of the parallel MPPT system must be designed, considering the operation condition under the highest current level, which occurs in the boost operation mode without solar irradiation (mode 5). The switching frequency was defined as equal to 30 kHz. The maximum power of the PV module is 45 Wp, and this value was considered in the design.

1) Inductor: The average inductor current in the boost operation is defined by (1), considering an efficiency equal to $\eta = 90\%$

$$I_{\mathrm{L}} = \frac{\mathrm{P}}{\mathrm{V_b} \cdot \eta} = \frac{45}{6 \cdot 0.9} = 8.333 \text{ A}. \tag{1}$$

A current ripple that is equal to 20% was considered in the inductance determination

$$\Delta I = 0.2 \cdot I_{\mathrm{L}} = 0.2 \cdot 8.333 = 1.667 \text{ A}. \tag{2}$$

The operation point defined is a duty cycle that is equal to $D = 0.67$, which is in order to obtain a load voltage that is equal to 18 V, with a battery voltage equal to 6 V. The inductance is calculated by

$$L = \frac{V_{\mathrm{in}} \cdot D}{f \cdot \Delta I} = \frac{6 \cdot 0.67}{30 \cdot 10^3 \cdot 1.667} = 80.4 \ \mu\text{H}. \tag{3}$$

An inductance value that is equal to 90 μH was utilized in the prototype.

2) Capacitor: A capacitor voltage ripple that is equal to 5% was adopted in the design of the filter capacitor

$$\Delta V_{\mathrm{C}} = V_o \cdot 0.05 = 18 \cdot 0.05 = 0.9 \text{ V}. \tag{4}$$

The capacitance is calculated by

$$C = \frac{I_{\mathrm{cap}} \cdot D}{f \cdot \Delta V_{\mathrm{C}}}. \tag{5}$$

The capacitor current is defined by

$$\begin{aligned} I_{\mathrm{cap}} &= I_{\mathrm{c}} + \frac{\Delta I}{2} \\ I_{\mathrm{cap}} &= \frac{45}{18} + \frac{1.667}{2} = 3.333 \text{ A}. \end{aligned} \tag{6}$$

Thus

$$C = \frac{3.333 \cdot 0.667}{30 \cdot 10^3 \cdot 0.9} = 82.337 \ \mu\text{F}. \tag{7}$$

Three capacitors with 33 μF/50 V were connected in parallel for the output capacitor implementation while also considering the equivalent series resistance.

3) Power Switches: The switch RMS current can be approximately defined by

$$I_{\mathrm{Srms}} = IL \cdot \sqrt{D} = 8.333 \cdot \sqrt{0.67} = 6.8 \text{ A}. \tag{8}$$

The power switch utilized in the prototype implementation was the MOSFET IRFZ48N.

E. Efficiency Analysis of the Parallel MPPT

The efficiency of the parallel MPPT can be analyzed by considering the different operation modes.

1) Efficiency for Operation Mode 2: Operation mode 2, which is shown in Fig. 12, occurs when the load current (I_{c}) is lower than the PV module MPP current (I_{mpp}). Thus, part of the energy generated is used to charge the battery. Therefore, the efficiency of the system is defined by (9), considering the PV module as the energy input, and the outputs are the load and battery

$$\eta(\%) = \frac{P_o}{P_{\mathrm{in}}} = \frac{P_{\mathrm{Load}} + P_{\mathrm{Battery}}}{P_{\mathrm{Module}}} = \frac{V_f \cdot I_{\mathrm{c}} + V_{\mathrm{Bat}} \cdot I_{\mathrm{Bat}}}{V_f \cdot I_f}. \tag{9}$$

2) Efficiency for Operation Mode 4: Operation mode 4, which is shown in Fig. 14, occurs when the load current (I_{c}) is higher than the PV module MPP current (I_{mpp}). Thus, part of the energy used by the load is supplied by the battery. Therefore, the efficiency of the system is defined by (10), considering the PV module and the battery as the energy inputs, and the output is the load

$$\begin{aligned} \eta(\%) &= \frac{P_o}{P_{\mathrm{in}}} \\ &= \frac{P_{\mathrm{Load}}}{P_{\mathrm{Module}} + P_{\mathrm{Battery}}} \\ &= \frac{V_f \cdot I_{\mathrm{c}}}{V_f \cdot I_f + V_{\mathrm{Bat}} \cdot I_{\mathrm{Bat}}}. \end{aligned} \tag{10}$$

3) Efficiency for Operation Mode 3: When the load current (I_{c}) is equal to the MPP current (I_{mpp}), corresponding to operation mode 3, the battery current (I_{Bat}) is zero. As shown in Fig. 13, the load current (I_{c}) is the same as the PV module current (I_f) when I_{b} is zero. Thus, substituting $I_f = I_{\mathrm{c}}$ and $I_{\mathrm{Bat}} = 0$ in (9) or (10), the efficiency is equal to 100%. In this case, all the energy generated is used by the load without losses, provided that there are ideal cables and connections.

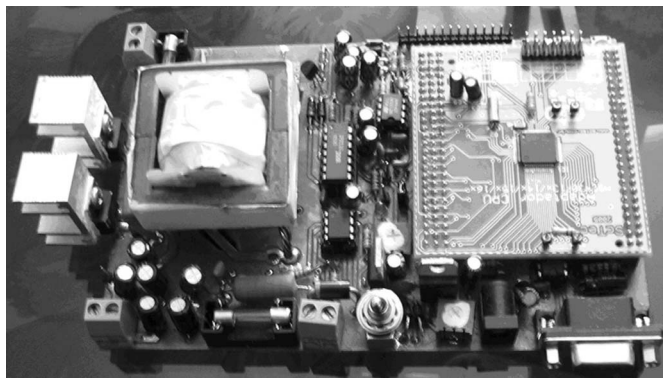

Fig. 17. Parallel MPPT laboratory prototype.

IV. Experimental Results

The operation of the proposed system was tested with the implementation of a laboratory prototype, which is shown in Fig. 17. The PV module utilized in the practical test was the Kyocera Solar KC40T with maximum power equal to 45 W.

A. MPPT Operation

The practical implementation of the control algorithms was accomplished with the microcontroller MSP430F149. The data acquisition was obtained through serial transmission from the

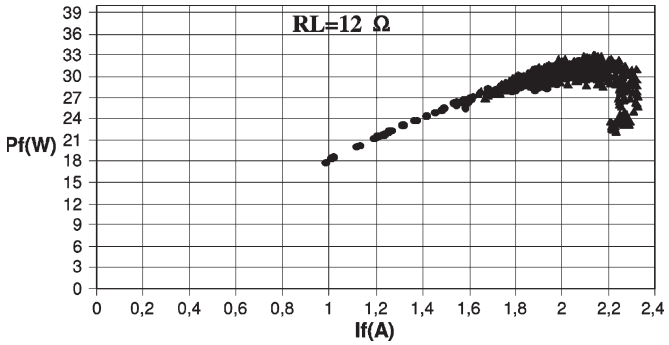

Fig. 18. Output power and current of the PV module.

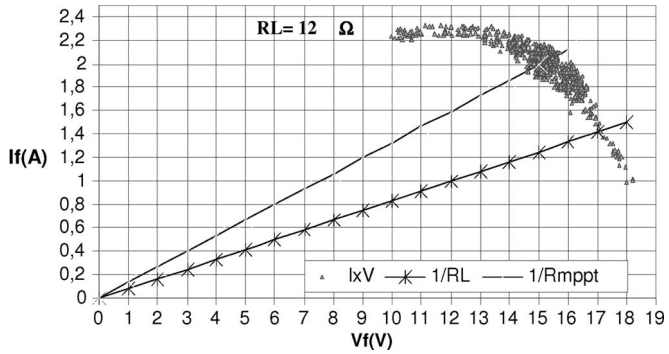

Fig. 19. Output current and voltage of the PV module.

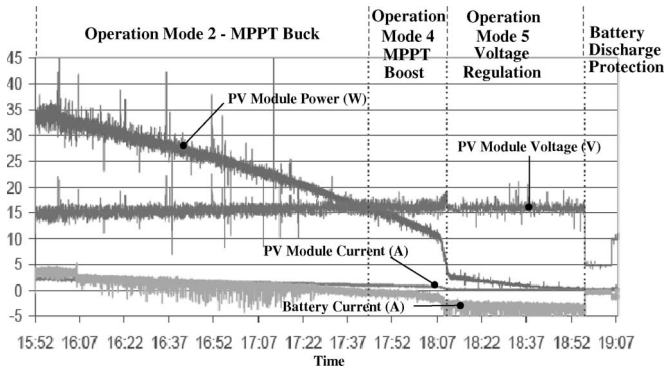

Fig. 20. Data acquisition of the parallel MPPT operation.

microcontroller to a computer. The main control information, such as voltage, current, power, and converter duty cycle, is stored during MPPT operation.

The experimental results of the MPPT system using the PV module KC40T are shown in Figs. 18–20, considering a load resistance that is equal to 12 Ω. Fig. 18 shows the PV module power and current.

The maximum power obtained for the climatic conditions was about 32 W, and the MPP current was equal to $I_{\mathrm{mpp}} = 2.1$ A. Fig. 19 shows the PV module output current and voltage curve, as well as two load lines. The lower line represents the connection of the load resistance directly to the PV module without the MPPT circuit.

The power obtained in this case was equal to 24 W. The upper line represents the equivalent load adjusted by the dc–dc converter and MPPT algorithm, obtaining a power that is equal

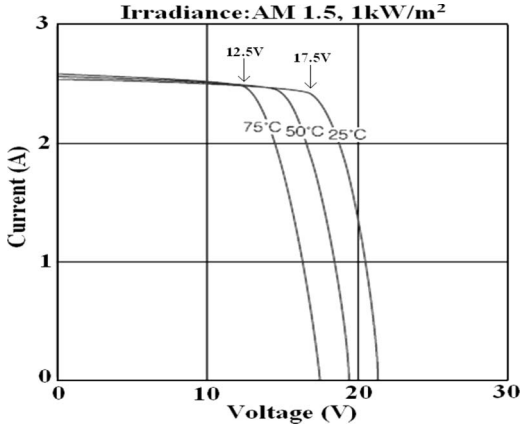

Fig. 21. PV module KC40T output as a function of temperature.

to 32 W. Thus, the 25% gain in power obtained with the MPPT was used to store energy in the battery.

Another test was carried out with the MPPT operating during a period of 3 h on a sunny day, and Fig. 20 shows the data obtained. This test shows the automatic transition between the different operation modes of the MPPT system. The test began at 15:52 h, and the energy generated by the PV module supplied the load and charged the battery, operating as a buck converter (operation mode 2). The battery current was positive during this operation mode. With the gradual reduction of solar irradiation, the power generated decreased. When the power generated by the PV module was lower than 15 W, the power circuit operated as a boost converter, and the power generated was complemented by battery energy (operation mode 4). The battery current was negative during this operation mode. At 18:07 h, solar irradiation was very low, and the power generated was almost zero. Thus, a voltage control loop regulated the output voltage, and only the battery energy supplied the load (operation mode 5). A low-capacity battery was used in order to show the discharge protection.

One hour after operation with the voltage regulation, the battery reached its minimal charge level, and the power converter was turned off. As shown in Fig. 20, the load voltage variation was low and was maintained at close to 15 V for all operation modes.

B. Output Voltage Variation

The PV module KC40T output characteristic, which is as a function of the temperature, is shown in Fig. 21. The MPP voltage changes from 17.5 V at 25 °C to 12.5 V at 75 °C. Therefore, a PV module temperature increase of 40 °C represents an MPP voltage reduction of 5 V. Solar irradiation does not present a significant influence on the MPP voltage. The MPPT algorithm ensures that the PV module operates at the MPP voltage for any climatic condition and load. Thus, the loads connected directly to the PV module (Fig. 3, "DC Load-1") must support the MPP voltage variation in the parallel MPPT system.

Fig. 22 shows the output voltage variation $(V_{\mathrm{Load}} - C2)$ for a load change from 5 to 10 Ω, using a classic perturbation and observation algorithm. When the load power and load current I_{c} were reduced in operation mode 2, the converter I_{b}, the

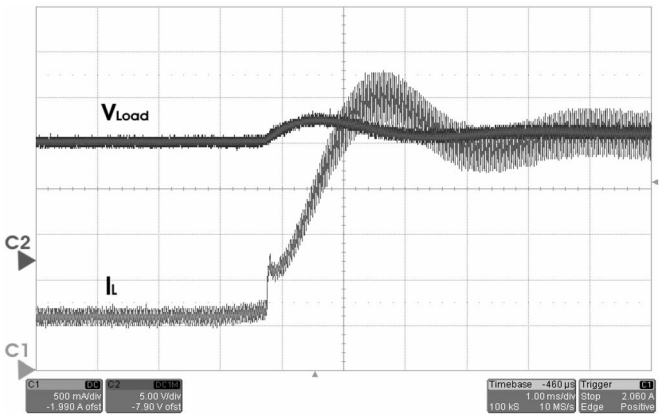

Fig. 22. (C2) Output voltage transient with load power reduction (0.5 A/div, 5 V/div, and 1 ms/div).

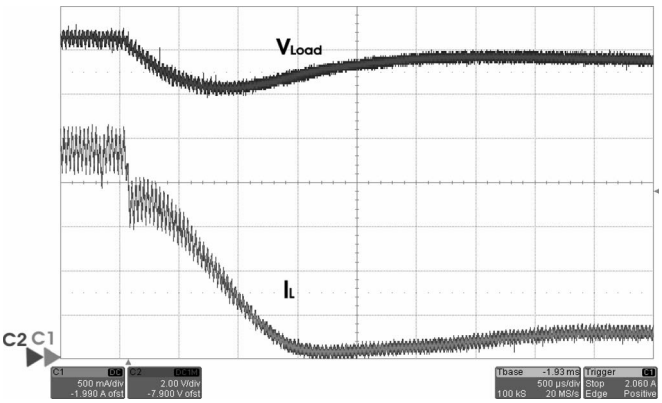

Fig. 23. (C2) Output voltage transient with load power increase (0.5 A/div, 2 V/div, and 0.5 ms/div).

battery charge, and the (C1) inductor $I_{\rm L}$ currents were increased in order to maintain the PV current at the MPP ($I_f = I_{\rm mpp} = I_{\rm b} + I_{\rm c}$). The output voltage variation in this case was about 3 V. Fig. 23 shows the load change from 10 to 5 Ω. With the increase of the load power and current $I_{\rm c}$, which is in operation mode 2, the converter $I_{\rm b}$, battery charge, and (C1) inductor $I_{\rm L}$ currents were decreased in order to maintain $I_f = I_{\rm mpp} = I_{\rm b} + I_{\rm c}$. The voltage variation in this transient was about 2.5 V. Loads whose voltage variation is critical can also be directly connected to the battery bank in the parallel system (Fig. 3, "DC Load-2"). However, as occurs in the series-connected system, the battery voltage can also change from the full charge to discharge states from 14.4 to 10.5 V.

C. Efficiency Experimental Results

Fig. 24 shows the series and parallel MPPT systems' efficiency curves obtained experimentally with the PV module KC40T. The MPP obtained with the parallel system (operation modes 2, 3, and 4) was equal to 32 W, as can be seen in Fig. 18. Thus, when the load power is equal to 32 W, the maximum system efficiency is reached because all the energy generated is transferred to the load (operation mode 3), and the power processed by the dc–dc converter is zero. Operation mode 2 occurs when the load power is lower than 32 W, and operation mode 4 occurs when the load power is higher than 32 W.

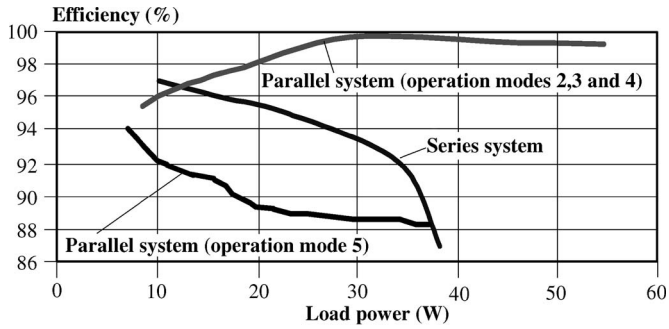

Fig. 24. Series and parallel MPPT systems efficiency.

Fig. 24 also shows the parallel MPPT system efficiency for operation mode 5, with the disconnection of the PV module. The bidirectional converter operates as a classical boost. However, it is important to highlight that the efficiency of the parallel MPPT system is always higher than the efficiency of the power converter.

In order to compare the measured efficiency of the proposed parallel MPPT system with the series-connected MPPT system, a buck dc–dc converter was implemented by using the same components and connecting the dc load, which is as presented in Fig. 2. The efficiency curve of the series-connected system is shown in Fig. 24. Efficiency decreased until it reached 87% at the MPP, which is equal to 38 W in this test. The parallel MPPT system efficiency was higher than the efficiency obtained with the series-connected system during PV power generation. However, considering dc load operation without solar irradiation, such as at night, the efficiency of the series-connected system is higher because the dc loads are directly connected to the battery while the parallel system presents the efficiency curve shown in Fig. 24. However, some specific loads, such as the lighting system, can be directly connected to the battery (Fig. 3, "DC Load-2") in order to reduce the disadvantage of the parallel system during the operation without solar irradiation. Therefore, in order to maximize the system efficiency, the dc loads should be properly shared between Load-1 and Load-2 (Fig. 3) on the basis of their prevalent use, i.e., during the day or during the night, respectively. When considering ac loads, the efficiency during operation without solar irradiation will be equivalent in the series and parallel connected systems because in both configurations, the step-up dc–dc converter efficiency must be considered.

V. Conclusion

An MPPT circuit with parallel connection is presented in this paper. The parallel connection of the MPPT system reduces the negative influence of power converter losses in the overall efficiency during PV power generation. The control algorithm ensures operation at the MPP as in the classical system; however, only a part of the power generated is processed by the dc–dc converter. The power converter implemented is multifunctional, operating as an MPPT circuit, battery charge, battery regulator, and step-up converter. A stand-alone generation system, with a reduced number of energy-processing stages, is proposed, allowing for the implementation of a high-efficiency PV

system. The main operational aspects of the parallel MPPT were verified with the implementation of a prototype. The transitions of the different operational modes were tested and occurred without any discontinuity of the system's operation.

REFERENCES

[1] E. V. Solodovnik, S. Liu, and R. A. Dougal, "Power controller design for maximum power tracking in solar installations," *IEEE Trans. Power Electron.*, vol. 19, no. 5, pp. 1295–1304, Sep. 2004.

[2] M. A. S. Masoum, S. M. M. Badejani, and E. F. Fuchs, "Microprocessor-controlled new class of optimal battery chargers for photovoltaic applications," *IEEE Trans. Energy Convers.*, vol. 19, no. 3, pp. 599–606, Sep. 2004.

[3] W. Xiao, N. Ozog, and W. G. Dunford, "Topology study of photovoltaic interface for maximum power point tracking," *IEEE Trans. Ind. Electron.*, vol. 54, no. 3, pp. 1696–1704, Jun. 2007.

[4] W. Xiao, W. G. Dunford, P. R. Palmer, and A. Capel, "Application of centered differentiation and steepest descent to maximum power point tracking," *IEEE Trans. Ind. Electron.*, vol. 54, no. 5, pp. 2539–2549, Oct. 2007.

[5] N. Femia, G. Petron, G. Spagnuolo, and M. Vitelli, "Optimization of perturb and observe maximum power point tracking method," *IEEE Trans. Power Electron.*, vol. 20, no. 4, pp. 963–973, Jul. 2005.

[6] M. G. Simões and N. N. Franceschetti, "Fuzzy optimisation based control of a solar array system," *Proc. Inst. Electr. Eng.—Electric Power Applications*, vol. 146, no. 5, pp. 552–558, Sep. 1999.

[7] J. A. Abu-Qahouq, H. Mao, H. J. Al-Atrash, and I. Batarseh, "Maximum efficiency point tracking (MEPT) method and digital dead time control implementation," *IEEE Trans. Power Electron.*, vol. 21, no. 5, pp. 1273–1281, Sep. 2006.

[8] N. Mutoh, M. Ohno, and T. Inoue, "A method for MPPT control while searching for parameters corresponding to weather conditions for PV generation systems," *IEEE Trans. Ind. Electron.*, vol. 53, no. 4, pp. 1055–1065, Aug. 2006.

[9] J. H. R. Enslin and D. B. Snyman, "Combined low-cost, high-efficient inverter, peak power tracker and regulator for PV applications," *IEEE Trans. Power Electron.*, vol. 6, no. 1, pp. 73–82, Jan. 1991.

[10] J. H. R. Enslin, M. S. Wolf, D. B. Snyman, and W. Swiegers, "Integrated photovoltaic maximum power point tracking converter," *IEEE Trans. Ind. Electron.*, vol. 44, no. 6, pp. 769–773, Dec. 1997.

[11] E. Koutroulis, K. Kalaitzakis, and N. C. Voulgaris, "Development of a microcontroller-based, photovoltaic maximum powerpoint tracking control system," *IEEE Trans. Power Electron.*, vol. 16, no. 1, pp. 46–54, Jan. 2001.

[12] R. J. Wai, W. H. Wang, and C. Y. Lin, "High-performance stand-alone photovoltaic generation system," *IEEE Trans. Ind. Electron.*, vol. 55, no. 1, pp. 240–250, Jan. 2008.

[13] T.-F. Wu, C.-H. Chang, and Y.-K. Chen, "A fuzzy-logic-controlled single-stage converter for PV-powered lighting system applications," *IEEE Trans. Ind. Electron.*, vol. 47, no. 2, pp. 287–296, Apr. 2000.

[14] Q. Li and P. Wolfs, "An analysis of the ZVS two-inductor boost converter under variable frequency operation," *IEEE Trans. Power Electron.*, vol. 22, no. 1, pp. 120–131, Jan. 2007.

[15] L. Schuch, C. Rech, H. L. Hey, H. A. Gründling, H. Pinheiro, and J. R. Pinheiro, "A battery ZVT bi-directional charger for uninterruptible power supplies," in *Proc. IEEE Power Electron. Spec. Conf.*, 2002, pp. 1841–1846.

Roger Gules was born in Bento Gonçalves, RS, Brazil, in 1971. He received the B.S. degree from the Federal University of Santa Maria, Brazil, and the M.S. and Ph.D. degrees from the Federal University of Santa Catarina, Florianopolis-SC, Brazil, in 1998 and 2001, respectively.

From 2001 to 2005, he was a Professor with the Universidade do Vale do Rio dos Sinos, São Leopoldo, Brazil. Since 2006, he has been with the Programa de Pós-Graduação em Engenharia Elétrica e Informática Industrial, Federal University of Technology CPGEI-UTFPR, Curitiba, Brazil, where he is a Professor. His research interests include high-frequency power conversion, power switching converters, and renewable energy applications.

Juliano De Pellegrin Pacheco was born in Criciúma, Brazil, in 1979. He received the B.S. degree in electrical engineering from the Federal Technological University of Paraná, Curitiba, Brazil, in 2004, where he is currently working toward the M.S. degree in the Programa de Pós-Graduação em Engenharia Elétrica e Informática Industrial.

His research interests include power electronics and renewable energy applications.

Hélio Leães Hey (S'90–M'91) was born in Santa Maria, Brazil, in 1961. He received the B.S. degree from The Catholic University of Pelotas, Pelotas, Brazil, in 1985, and the M.S. and Ph.D. degrees from the Federal University of Santa Catarina, Florianopolis-SC, Brazil, in 1987 and 1991, respectively.

From 1989 to 1993, he was with the Federal University of Uberlândia, Uberlândia, Brazil. From 2005 to 2006, he was with the Electrical and Electronic Department of the University of Oviedo, Oviedo, Spain, where he performed his postdoctoral research on power-factor-correction and soft-switching techniques. Since 1994, he has been with the Power Electronics and Control Research Group, Federal University of Santa Maria, Santa Maria, where he is currently a Professor. He has authored more than 140 papers published in power electronics journals and conference proceedings. From 1995 to 1999, he was the Editor of the *Brazilian Power Electronics Journal*. His research interests include soft-switching techniques, high-frequency power conversion, power-factor-correction techniques, and renewable energy applications.

Dr. Hey is a member of the Brazilian Power Electronics Society and the Brazilian Automatic Control Society.

Johninson Imhoff was born in São Miguel do Oeste, SC, Brazil, in 1979. He received the B.S. and M.S. degrees in electrical engineering from the Federal University of Santa Maria, Santa Maria, Brazil, in 2004 and 2007, respectively.

He is currently a Product Development Engineer with Electrolux do Brazil S.A., Curitiba, Brazil. His research interests include photovoltaic systems, and power-factor-correction and motor-control techniques.

Mr. Imhoff is a member of the Brazilian Power Electronics Society.